Cancer Pathogenesis and Therapy 2 (2024) 38–49

Contents lists available at ScienceDirect

Cancer Pathogenesis and Therapy

journal homepage: www.journals.elsevier.com/cancer-pathogenesis-and-therapy

Research article

Reversal of the immunosuppressive tumor microenvironment via platinum-based neoadjuvant chemotherapy in cervical cancer

Xue Feng [a,b,1], Xiaolin Meng [a,b,1], Dihong Tang [c,1], Shuaiqingying Guo [a,b], Qiuyue Liao [a,b], Jing Chen [a,b], Qin Xie [a,b], Fengyuan Liu [a,b], Yong Fang [a,b], Chaoyang Sun [a,b], Yingyan Han [a,b,***], Jihui Ai [a,b,**], Kezhen Li [a,b,*]

[a] Department of Gynecological Oncology, Tongji Hospital, Tongji Medical College, Huazhong University of Science and Technology, Wuhan, Hubei 430000, China
[b] National Clinical Research Center for Obstetrics and Gynecology, Cancer Biology Research Center (Key Laboratory of the Ministry of Education), Tongji Hospital, Tongji Medical College, Huazhong University of Science and Technology, Wuhan, Hubei 430000, China
[c] Department of Gynecologic Oncology, Hunan Cancer Hospital/The Affiliated Cancer Hospital of Xiangya School of Medicine, Central South University, Changsha, Hunan 410000, China

HIGHLIGHTS

- Treatment-naive cervical cancer demonstrates an *in situ* immunosuppressive tumor microenvironment.
- Neoadjuvant chemotherapy (NACT) can powerfully reduce regulatory T cells and indoleamine 2,3-dioxygenase positive (IDO^+) cells.
- NACT enhances antigen presentation in responders and promotes effector T-cell infiltration.
- NACT promotes major histocompatibility complex-mediated antigen presentation in cervical cancer immune microenvironment.

GRAPHICAL ABSTRACT

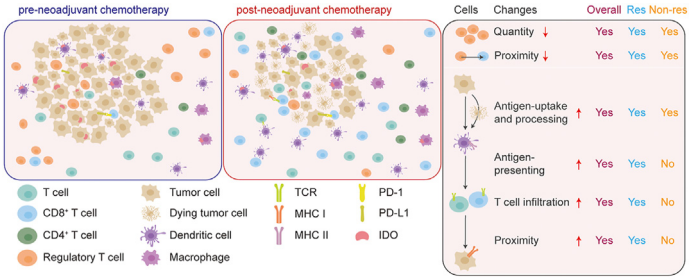

Immunological changes induced by neoadjuvant chemotherapy in cervical cancer. CD: Cluster of differentiation; Downward arrow: Decreased or weakened; IDO: Indoleamine 2,3-dioxygenase; MHC: Major histocompatibility complex; Non-res: Non-responders; PD-1: Programmed cell death 1; PD-L1: Programmed cell death 1 ligand 1; Res: Responders; TCR: T cell receptor; Upward arrow: Increased or enhanced.

ARTICLE INFO

Managing Editor: Peng Lyu

Keywords:
Neoadjuvant chemotherapy
Cervical cancer
Tumor immune microenvironment

ABSTRACT

Background: Immunotherapy favors patients with tumors; however, only 3–26.3% of patients with cervical cancer benefit from single-agent immune checkpoint inhibitors. Combined immunotherapy and chemotherapy has been explored against tumor; however, the combination remains controversial. This study aimed to investigate the tumor immune microenvironment (TIME) and the effects of platinum-based neoadjuvant chemotherapy (NACT) in cervical cancer to identify the clinical value of combining chemotherapy with immunotherapy.

* Corresponding author: Department of Gynecological Oncology, Tongji Hospital, Tongji Medical College, Huazhong University of Science and Technology, Wuhan, Hubei 430000, China.
** Corresponding author: Department of Gynecological Oncology, Tongji Hospital, Tongji Medical College, Huazhong University of Science and Technology, Wuhan, Hubei 430000, China.
*** Corresponding author: Department of Gynecological Oncology, Tongji Hospital, Tongji Medical College, Huazhong University of Science and Technology, Wuhan, Hubei 430000, China.
E-mail addresses: hanyingyan1222@163.com (Y. Han), jihuiai@tjh.tjmu.edu.cn (J. Ai), tjkeke@126.com (K. Li).
[1] Xue Feng, Xiaolin Meng, and Dihong Tang contributed equally to this work.

https://doi.org/10.1016/j.cpt.2023.07.003
Received 13 May 2023; Received in revised form 13 July 2023; Accepted 21 July 2023

Spatial architecture
CD8
Regulatory T cells

Methods: Multiplex immunohistochemistry (IHC) with 11 markers (cluster of differentiation [CD]3, CD8, CD4, CD11c, CD68, forkhead box P3 [Foxp3], programmed cell death 1 [PD-1], programmed cell death 1 ligand 1 [PD-L1], indoleamine 2,3-dioxygenase [IDO], cyclin-dependent kinase inhibitor 2A [p16], and cytokeratin [CK]) was performed to evaluate TIME from 108 matched pre- and post-NACT cervical cancer samples. The mechanism of antitumor immunity triggered by NACT was explored using RNA sequencing (RNA-seq) from four paired samples and subsequently verified in 41 samples using IHC.

Results: The infiltration rate of the $CD8^+$ T cells in treatment-naive cervical cancer was 0.73%, and those of $Foxp3^+$ regulatory T cells (Tregs) and IDO^+ cells were 0.87% and 17.15%, respectively. Moreover, immunoreactive T cells, dendritic cells, and macrophages were more in the stromal than the intratumor region. NACT increased dendritic, $CD3^+$ T, $CD8^+$ T, and $CD4^+$ T cells and decreased Tregs. The aforementioned alterations occurred predominantly in the stromal region and were primarily in responders. Non-responders primarily showed decreased Tregs and no increase in $CD8^+$ T or dendritic cell infiltration. Furthermore, dendritic cells interacted more closely with $CD3^+$ T cells after NACT, an effect primarily observed in responders. RNA-seq data revealed activation of the antigen receptor-mediated signaling pathway and upregulation of major histocompatibility complex (MHC) I and MHC II after chemotherapy, validated using IHC.

Conclusions: NACT can reduce Tregs, and when tumor cells are effectively killed, antigen presentation is enhanced, subsequently activating antitumor immunity finitely. Our study provides the molecular characteristics and theoretical basis for the simultaneous or sequential combination of platinum-based NACT and immunotherapy for cervical cancer.

Introduction

The immunosuppressive tumor microenvironment is essential for tumorigenesis, development, and treatment and has received increasing attention annually.[1,2] Therefore, evaluating immune infiltration in a specific tumor microenvironment is conducive to a deeper understanding of the mechanisms of tumor development. Similarly, antitumor immunotherapy, including cytokines, therapeutic vaccines, antibodies, and adoptive cell therapy (ACT), has gradually become possible, with excellent results achieved in tumor therapy. For example, rituximab has revolutionized the treatment of B-cell malignancies.[3] Immune checkpoint inhibitors (ICIs) targeting PD-1/PD-L1 are currently the care standard for 16 cancer types and tissue-agnostic indications.[4] Moreover, ACT has recently achieved durable clinical responses in otherwise treatment-refractory cancers.[5] However, the effects of antitumor immunotherapy vary across cancer types. The objective response rate of PD-1/PD-L1 inhibitors in Hodgkin's lymphoma and desmoplastic melanoma has reached 70% or >80%[6,7]; however, patients with pancreatic or prostate cancer lesions rarely benefit from the current ICIs.[8,9] These enormously different responses to immunotherapy within and between tumor types may be related to the heterogeneity in tumor-intrinsic features, particularly the tissue-specific immune microenvironment.[1,10,11] Therefore, comprehensive analyses of the immune infiltration of the tumor are urgent to optimize immunotherapy application.

With the improved treatment, the 5-year survival rate of cervical cancer has reached approximately 70%; however, it has improved insignificantly since the 1970s.[12–14] The primary etiological factor in cervical cancer is persistent human papillomavirus (HPV) infection, which is favorable in cervical cancer immunotherapy owing to the presence of a specific tumor antigen.[15] Therefore, many immunotherapeutic approaches have been adopted for cervical cancer. Tumor-infiltrating lymphocytes selected for HPV oncogenes E6 and E7 reportedly cause tumor regression in patients with metastatic cervical cancer.[16] However, the responses of single-agent ICIs in cervical cancer are modest, ranging from 3 to 26.3%.[17] Hence, combining immunotherapy with traditional treatments has attracted many researchers. Combined immunotherapy and chemotherapy has been approved for various indications, although the clinical data show different therapeutic effects, such as in non-small cell lung and triple-negative breast cancers.[18–20] In cervical cancer, combining pembrolizumab with chemotherapy achieved better survival.[21] Nevertheless, the controversy over combining chemotherapy and immunotherapy has been constant, primarily focusing on the killing effect of chemotherapy on immune cells and the regulation of the local tumor immune microenvironment (TIME),[22] which require investigation to help advance immunotherapy in cervical cancer and facilitate developing novel therapeutic strategies.

Zhang et al. found that neoadjuvant chemotherapy (NACT)-treated cervical cancer experienced a significant increase in CD8 positivity[23]; however, Liang et al. observed stable CD8 expression pre- and post-NACT.[24] The assessments in these studies rely on individual markers rather than their combinations, ignoring the interactions between immune and tumor cells. As immunity typically functions based on intercellular contacts and short-distance cytokine communications, the location and spatial relationships of the TIME can enhance understanding of the biology and potential predictive biomarkers of disease outcomes.[25,26] Multiplex immunohistochemistry (mIHC), emerging as an *in situ* single-cell and spatial analysis technique, has been used to portray the spatial immunophenotype with more accurate identification of immune cells by multiple markers on the same cell. Accumulating studies have suggested the significance of the immune cell spatial distribution, such as short overall survival in lung cancer with a high regulatory T cell (Tregs) density around tumor cells.[27] However, few studies have intensively scrutinized the spatial immunophenotype of cervical cancer, and understanding treatment-induced longitudinal changes in tumor immune architecture can provide potential predictive information guiding therapeutic decision-making.

Based on these insights, we systematically surveyed the immunological properties at the tumor site at baseline and upon platinum-based NACT in cervical cancer using 7-color mIHC. These integrated analyses will consolidate the theoretical basis for promoting immunotherapy with or without combined chemotherapy for cervical cancer.

Methods

Patient cohort

Detailed information is provided in Supplementary Figure 1. The retrospectively collected formalin-fixed and paraffin-embedded (FFPE) sections from patients with cervical cancer receiving NACT in Tongji Hospital between January 2015 and June 2021 and Hunan Cancer Hospital between February 2013 and August 2019 were assessed with mIHC and immunohistochemistry (IHC). For RNA sequencing (RNA-seq) analysis, four matched fresh tumor tissues were collected and assayed. All patients underwent 1–2 cycles of NACT with platinum and taxanes, followed by radical hysterectomy or concurrent chemoradiotherapy.

Neoadjuvant chemotherapy response evaluation

The cancer stage was determined through pelvic examination by two expert gynecologic oncologists. The clinical response to NACT was

evaluated based on the imaging data (B-ultrasound/computed tomography [CT]/magnetic resonance imaging [MRI]) before and after NACT according to the response evaluation criteria in solid tumors guidelines version 1.1 (RECIST1.1).[28] Complete response (CR) was defined as the disappearance of the initial lesion. Partial response (PR) was defined as at least a 30% reduction in the sum of the longest dimensions of the primary tumors. An increase in the sum of the longest dimensions by at least 20% or the emergence of new lesions indicated progressive disease (PD). A case falling between PR and PD was termed stable disease (SD). Patients with CR or PR were classified as NACT responders, whereas those with SD or PD were the non-responders.

Multiplex immunohistochemistry (mIHC) staining, imaging, and quantification

mIHC was performed on 4-μm-thick FFPE sections using the Opal multiplex IHC Kit (PerkinElmer, NEL797001KT) and the PANO 7-plex IHC kit (TSA-RM). Briefly, tissue sections were deparaffinized, hydrated, and fixed for 20 min with a 10% neutral formalin solution (BBI, E672001). AR6 or Tris-ethylenediaminetetraacetic acid (Tris-EDTA) buffer was used for antigen retrieval. The slides were blocked with goat serum (Boster Bio, AR0009) for 30 min and incubated with the primary antibody for 1 h at 25 °C [Supplementary Table 1]. Subsequently, the horseradish peroxidase (HRP)-conjugated secondary antibody (PerkinElmer, NEL797001KT) was added for 30 min, followed by incubation with tyramide signal amplification (TSA) fluorochromes for 10 min, both at 25 °C. These steps were repeated for each primary antibody. Finally, the slides were counterstained with 4′,6-diamidino-2-phenylindole (DAPI) and mounted with Fluoromount-G (SouthernBiotech).

Multiplex-stained tissue slides were scanned using Vectra 3.0 software (PerkinElmer, USA), and the raw high-power fields of each sample were acquired for further analysis. An algorithm including spectral unmixing, tissue segmentation, cell segmentation, and score [Supplementary Figure 2] was built using inForm 2.4 software (PerkinElmer, USA) and applied to batch analysis of all images. The regional percentage of certain cells was calculated as the ratio of the targeted cell count to the total cell count. For cell spatial localization analyses, the intercellular distance was computed as the mean distance of each center cell to its nearest immune cell. Intercellular interactions were defined as the number of immune cells neighboring the center cell within a given distance.

Immunohistochemistry staining and quantification

As described above, the FFPE sections were deparaffinized and hydrated, and antigens were retrieved with Tris-EDTA buffer. Endogenous peroxidase activity was quenched with 3% H_2O_2. After blocking with goat serum, the slides were incubated with primary antibodies [major histocompatibility complex (MHC) I, ab134189/Abcam, 1:2000 or MHC II, ab170867/Abcam, 1:300], followed by incubation with HRP-conjugated secondary antibodies (AntGene, ANT020). Immunoperoxidase staining was performed using the 3,3′-diaminobenzidine (DAB) system (Servicebio, G1212). Finally, the slides were counterstained with hematoxylin and coverslipped with a mounting solution. The results were recorded using a TEKSQRAY scanner (SQS-40R) and quantified by three pathologists. The staining score was calculated as the area score × intensity score. Area scores were graded as 0–25% (1), 26–50% (2), 51–75% (3), and 76–100% (4); intensity scores were graded as negative (0), weakly positive (1), positive (2), and strongly positive (3).

Ribonucleic acid sequencing and analysis

The specimens were soaked in RNAlater (Thermo Fisher Scientific), preserved immediately, and sequenced by BGI-Shenzhen (China). The complementary deoxyribonucleic acid (cDNA) library was constructed using the BGISEQ-500 platform. The obtained clean reads were compared to the reference genome sequence (reference genome version: GCF_000001405.39_GRCh38.p13) using hierarchical indexing for spliced alignment of transcripts (HISAT), and gene expression levels were obtained for subsequent analysis. The immune cell infiltration in each sample was evaluated using TIMER.2 (http://timer.comp-genomics.org/).[29] Gene set enrichment analysis (GSEA) was used to analyze the changes in pathways. The sequencing data in this study have been deposited in the National Center for Biotechnology Information Sequence Read Archive under accession number SRP405747.

Statistical analysis

Statistical analyses were performed using R software (version 4.1.1) and GraphPad Prism 8 (GraphPad Software, USA). Changes before and after NACT were analyzed using the Wilcoxon signed-rank test. All P values were two-sided, and statistical significance was set at $P < 0.05$.

Results

Pre-neoadjuvant chemotherapy tumor microenvironment of cervical cancer shows an immunosuppressive state

To systematically analyze the TIME of cervical cancer, we performed two panels of mIHC staining using 11 markers (CD3, CD8, CD4, CD11c, CD68, Foxp3, PD-1, PD-L1, IDO, p16, and CK) in 108 matched pre- and post-NACT samples [Figure 1A and B and Table 1]. All patients received one (57 patients) or two (51 patients) cycles of platinum-based NACT, and the differences found in the proportion of different clinical responses between them were insignificant ($P = 0.15$, Supplementary Figure 3). We evaluated the immune microenvironment of the intratumor, stromal, and whole sample regions [Supplementary Figure 2].

The median proportions of $CD3^+$ T (pan T cells) and $CD8^+$ T cells in cervical cancer were 6.69% and 0.73%, respectively, whereas those of $CD4^+$ helper cells and $Foxp3^+$ Tregs were 1.14% and 0.87%, respectively. In addition, the infiltration rates of $CD11c^+$ dendritic cells and $CD68^+$ macrophages were 2.2% and 2.5%, respectively. Cells positive for IDO, which inhibits antitumor immunity at high expression, showed a 17.15% rate. Furthermore, 65.3% of dendritic cells and 34.36% of macrophages expressed IDO, representing cells with immunosuppressive regulation. PD-L1 (1.50%) and PD-1 (0.11%) levels were relatively low in the samples [Figure 1C and D]. Although the expression levels of each immune marker differed significantly, correlation analysis showed that the immune molecules are co-expressed in cervical cancer [Figure 1E]. Moreover, all T cell, dendritic cell, and macrophage types could not be concentrated in the intratumor region; however, they were primarily distributed in the stromal region (stromal region *vs.* intratumor region: CD3, 14.46% *vs.* 2.77%; CD8, 1.32% *vs.* 0.23%; CD4, 3.31% *vs.* 0.21%; Foxp3, 1.82% *vs.* 0.36%; CD11c, 3.19% *vs.* 1.86%; and CD68, 3.18% *vs.* 2.36%). Similarly, PD-1 was primarily expressed in the stromal region (0.18% *vs.* 0.07%). However, the expression levels of PD-L1 (1.16% *vs.* 1.24%) and IDO (14.41% *vs.* 15.65%) were relatively higher in the intratumor region [Figure 1F]. In summary, the treatment-naive TIME in cervical cancer lacked effective antitumor immune cell infiltration.

Neoadjuvant chemotherapy increases antitumor immune cells and decreases immunosuppressive cells

The infiltration of macrophages and $CD3^+$ T, $CD8^+$ T, $CD4^+$ T, and $CD11c^+$ dendritic cells increased significantly, suggesting activated antitumor immunity after chemotherapy [Figure 2A]. However, evident enrichment of CD3, CD8, CD4, CD11c, and CD68 occurred in the stromal rather than the intratumor region, where immune cell infiltration remained unabundant [Figure 2B and C]. In addition, the overall change in PD-1 was unnoticeable, while a differential distribution change (an increase in the intratumor region and a decrease in the stromal region) was observed. However, the $PD\text{-}1^+CD8^+$ T/$CD8^+$ T cells in the intratumor

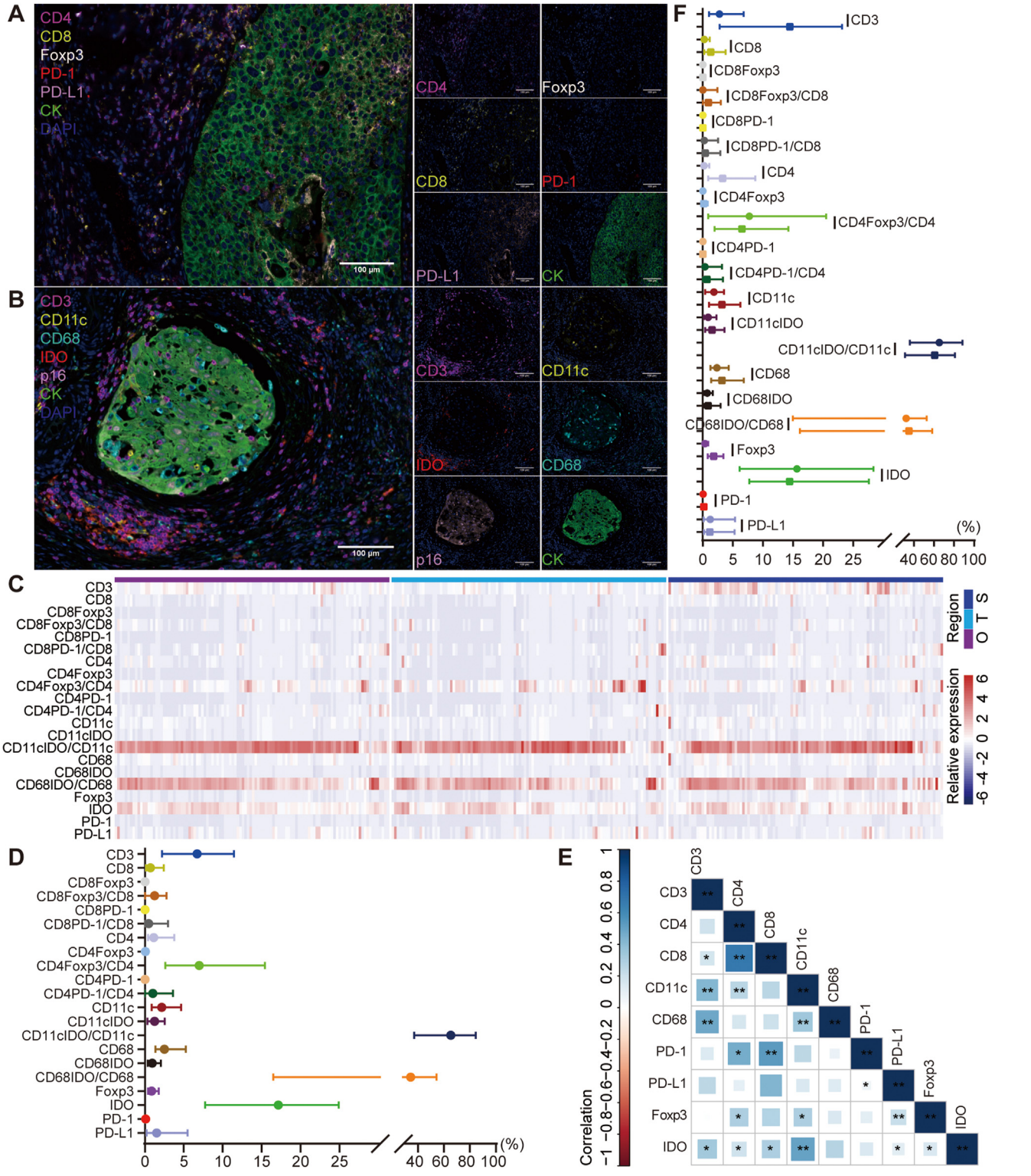

Figure 1. Seven-color multiplex staining identified immune cells from 108 human cervical cancer tissues. Representative composite image of the sample with (A) panel 1 and (B) panel 2 staining and the individual markers. Scale bar, 100 μm. (C) Heatmap showing the percentage of all the markers in the overall (O, left), intratumor (T, middle), and stromal (S, right) regions of tumors at baseline. (D) The percentage of immune markers in cervical cancers among the overall region. All data are displayed as median with 25th–75th percentiles. (E) Correlation matrix of evaluated immune markers among the overall region. *$P < 0.05$, **$P < 0.01$. (F) The percentage of immune markers in cervical cancers among the intratumor (circle), and stromal (square) regions. All data are displayed as median with 25th–75th percentiles. CD4: Helper T cells; CD8: Cytotoxic T lymphocytes; CD: Cluster of differentiation; CK: Cytokeratin; DAPI: 4',6-Diamidino-2-phenylindole; Foxp3: Forkhead box P3; IDO: Indoleamine 2,3-dioxygenase; p16: Cyclin-dependent kinase inhibitor 2A; PD-1: Programmed cell death 1; PD-L1: Programmed cell death 1 ligand 1.

Table 1
Characteristics of the 108 patients with cervical cancer with samples being subjected to multiplex immunohistochemistry staining.

Characteristics	Category	*N* (%)
Age (years), median (range)	–	50 (30–67)
FIGO Stage	IB3	28 (25.9)
	IIA2	35 (32.4)
	≥IIB	45 (41.7)
Histopathology	Squamous cell carcinoma	98 (90.7)
	Adenocarcinoma	8 (7.4)
	Neuroendocrine carcinoma	2 (1.9)
Histological grade	I	2 (1.9)
	II	62 (57.4)
	III	39 (36.1)
	Unknown	5 (4.6)
Tumor diameters (cm), median (range)	–	4.8 (1.9–10.3)
	<4	28 (25.9)
	≥4	80 (74.1)
Stromal Invasion	<1/3	6 (5.6)
	≥1/3, <2/3	46 (42.6)
	≥2/3	56 (51.8)
Lymphovascular space invasion	Positive	12 (11.1)
	Negative	96 (88.9)
Lymph node metastasis	Yes	29 (26.9)
	No	79 (73.1)
Uterine corpus metastasis	Yes	7 (6.5)
	No	101 (93.5)
Parametrial involvement	Positive	2 (1.9)
	Negative	106 (98.1)
Cycle of NACT	1 cycle	56 (51.9)
	2 cycles	52 (48.1)
Clinical response to NACT	CR	10 (9.2)
	PR	66 (61.1)
	SD	32 (29.6)

CR: Complete response; FIGO: International Federation of Gynecology and Obstetrics; NACT: Neoadjuvant chemotherapy; PR: Partial response; SD: Stable disease.

region differed insignificantly, suggesting that T cell exhaustion in the intratumor region was unaffected by chemotherapy [Figure 2B]. PD-L1 changed insignificantly in the intratumor region and declined in the stromal. Similarly, the relative percentage of Tregs with immunosuppressive functions, including total, $CD8^+$, and $CD4^+$ Tregs, decreased significantly after chemotherapy in the stromal and intratumor regions [Figure 2A–C and Supplementary Figure 4]. Moreover, IDO showed a notable downward trend, and this change was primarily concentrated in the stromal region. The proportion of IDO^+CD11c^+ dendritic cells in total $CD11c^+$ dendritic cells decreased, particularly in the stromal region, despite the augmentation of $CD11c^+$ dendritic cells in the stromal and intratumor regions, indicating impairment in inhibitory dendritic cells and enhancement in those with antigen presentation ability after chemotherapy [Figure 2A–C and Supplementary Figure 5]. Representative mIHC images in the 108 cases with matched pre- and post-NACT sections are shown in Figure 2D and E. These data indicate that NACT reduced immunosuppressive cells and increased antitumor immune cells in cervical cancer, fostering pronounced immune augmentation.

Reversal of the immunosuppressive microenvironment is more evident in responders than in non-responders

We analyzed the immune response of patients with different clinical responses. Consistent with previous results, $CD3^+$ T, $CD8^+$ T, $CD4^+$ T, and $CD11c^+$ dendritic cells increased significantly in NACT responders, particularly in the stromal region [Figure 3A–C]. Furthermore, the $CD8^+PD\text{-}1^+$ cells increased with increased CD8 in the intratumor region, while their proportion out of total $CD8^+$ T cells remained stable, implying no NACT influence on $CD8^+$ T cell exhaustion [Figure 3B]. However, the proportion of $CD8^+PD\text{-}1^+$ T cells in the overall and stromal regions decreased, possibly related to the inadequate antigenic stimulation of $CD8^+$ cells in the stromal region [Figure 3A and C]. As the PD-1 ligand and an essential ICIs target, PD-L1 changed insignificantly and only slightly decreased in the stromal region [Figure 3A–C]. The proportion of total, $CD4^+$, and $CD8^+$ Tregs decreased considerably after NACT in the intratumor and stromal regions [Figure 3A–C]. Similarly, NACT reduced IDO expression and the proportion of IDO^+ dendritic cells out of total dendritic cells, particularly in the stromal region. Given the increased total dendritic cells, assuming that responders acquired more activated dendritic cells with stronger tumor antigen presentation was reasonable.

In non-responders, the changes in immune cell infiltration mentioned above were relatively weaker. Except for the increased $CD4^+$ T cell infiltration, other immune cells, including $CD3^+$ T cells, $CD8^+$ T cells, dendritic cells, and macrophages, showed statistically insignificant differences post-NACT. NACT did not alter the expression of immunomodulatory molecules, including PD-1, PD-L1, and IDO. Consistent with responders, NACT significantly reduced the proportions of the total, $CD4^+$, and $CD8^+$ Tregs and those of inhibitory dendritic cells out of total dendritic cells. NACT effectively reduces immunosuppressive T cells in non-responders, causing notable infiltration of immunoreactive cells dominated by $CD8^+$ T cells and activated dendritic cells in addition to Tregs reduction in responders, depicted in Figure 3D and E by representative mIHC images from responders and non-responders.

Neoadjuvant chemotherapy induces antitumor immune cells to approach and act on tumor cells while driving out tumor-promoting immune cells

The distance between cancer and immune cells [Figure 4A] and the number of immune cells within a certain radius around each tumor cell [Figure 4B] showed a visible spatial architecture of TIME to further explore the crosstalk between immune and cancer cells.[30] In pre-NACT cases, many immune cell types were primarily over 100 μm away from tumor cells. However, cells expressing IDO, capable of suppressing activated tumor-reactive T cells, were enriched around the tumor cells within 73–152 μm [Figure 4C and Supplementary Figure 6]. This was consistent with the number of immune cells; that is, the stromal region was relatively rich in immune cells, while the intratumor region had a relatively high expression of immune inhibitory markers.

NACT induced the migration of macrophages and $CD3^+$ T, $CD8^+$ T, $CD4^+$ T, and dendritic cells toward tumor cells, with $CD3^+$ T cells from 121 to 89 μm, $CD8^+$ T cells from 214 to 152 μm, and $CD4^+$ T cells, dendritic cells, and macrophages from 221, 180, and 150 μm to 164, 125, and 104 μm, respectively [Figure 4C]. Their increased numbers within 15–50 μm of the tumor cells suggested that these cells, particularly $CD8^+$ T cells, attempted interacting with the tumor cells [Figure 4D]. In contrast, total (205–286 μm), $CD8^+$ (380–750 μm), and $CD4^+$ (288–347 μm) Tregs diverged from tumor cells post-NACT [Figure 4C], and the total number of Tregs around the tumor cells decreased accordingly [Figure 4D]. However, although IDO^+ cells approached tumor cells more, and the IDO-expressing dendritic cells and macrophages around the tumor cells increased, their proportions out of total dendritic cells and macrophages decreased continuously, indicating immune activation [Figure 4C and Supplementary Table 2].

NACT notably reduced $Foxp3^+$ cells around tumor cells within 50 μm and significantly increased the distance between them in responders and non-responders [Figure 4E and F]. Conversely, in responders, NACT induced the aggregation of $CD3^+$, $CD8^+$, $CD11c^+$, and $CD68^+$ cells around tumor cells [Figure 4E]. Dendritic, $CD68^+$, and $CD4^+$ cells increased within 50 μm of tumor cells, suggesting the activation of antigen uptake and processing; the number of $CD3^+$ and $CD8^+$ T cells particularly increased significantly, indicating that NACT enhanced $CD8^+$ T cell recruitment to kill tumor cells, consistent with increased $PD\text{-}1^+CD8^+$ cells within 50 μm around the tumor cells [Figure 4F]. Non-responders showed a similar trend; however, no statistical differences in $CD3^+$ or $CD8^+$ T cells. Therefore, NACT successfully broke the immunosuppressive spatial architecture in cervical cancer because it dispersed immunosuppressive cells and recruited more antigen uptake

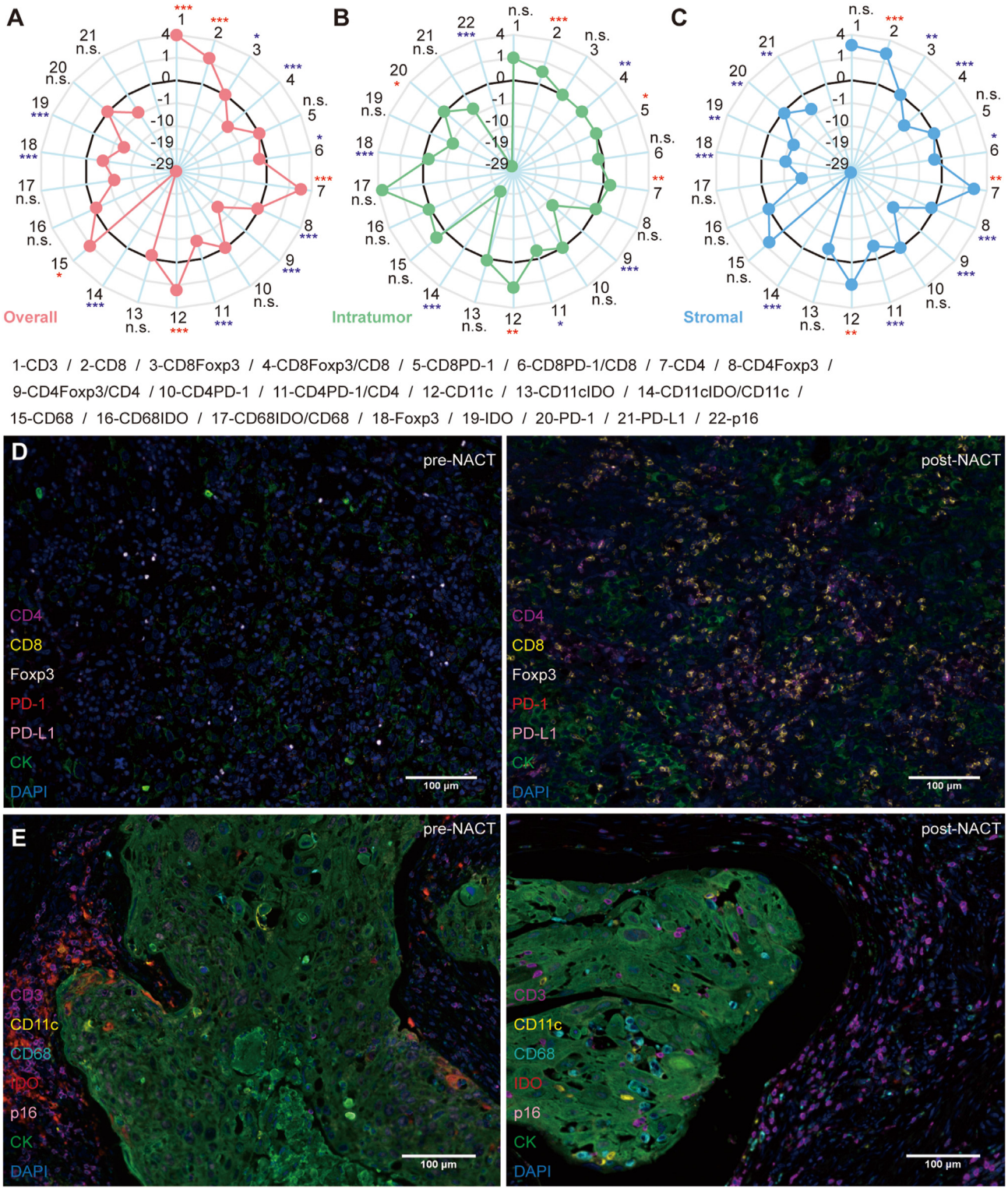

Figure 2. Neoadjuvant chemotherapy (NACT) caused an altered immune microenvironment in cervical cancer. The change of each immune marker in pre- and post-NACT tumor samples across the (A) overall, (B) intratumor, and (C) stromal regions. Representative images of multiplex staining in paired pre- and post-NACT cervical cancer samples with (D) panel 1 and (E) panel 2. n.s. $P \geq 0.05$, $^{*}P < 0.05$, $^{**}P < 0.01$, $^{***}P < 0.001$. *P* values were acquired using the Wilcoxon signed-rank test. The red marks represent a significant increase, while the blue represents a significant decrease in infiltration. CD: Cluster of differentiation; CK: Cytokeratin; DAPI: 4′,6-Diamidino-2-phenylindole; Foxp3: Forkhead box P3; IDO: Indoleamine 2,3-dioxygenase; NACT: Neoadjuvant chemotherapy; n.s.: Non-significant; p16: Cyclin-dependent kinase inhibitor 2A; PD-1: Programmed cell death 1; PD-L1: Programmed cell death 1 ligand 1.

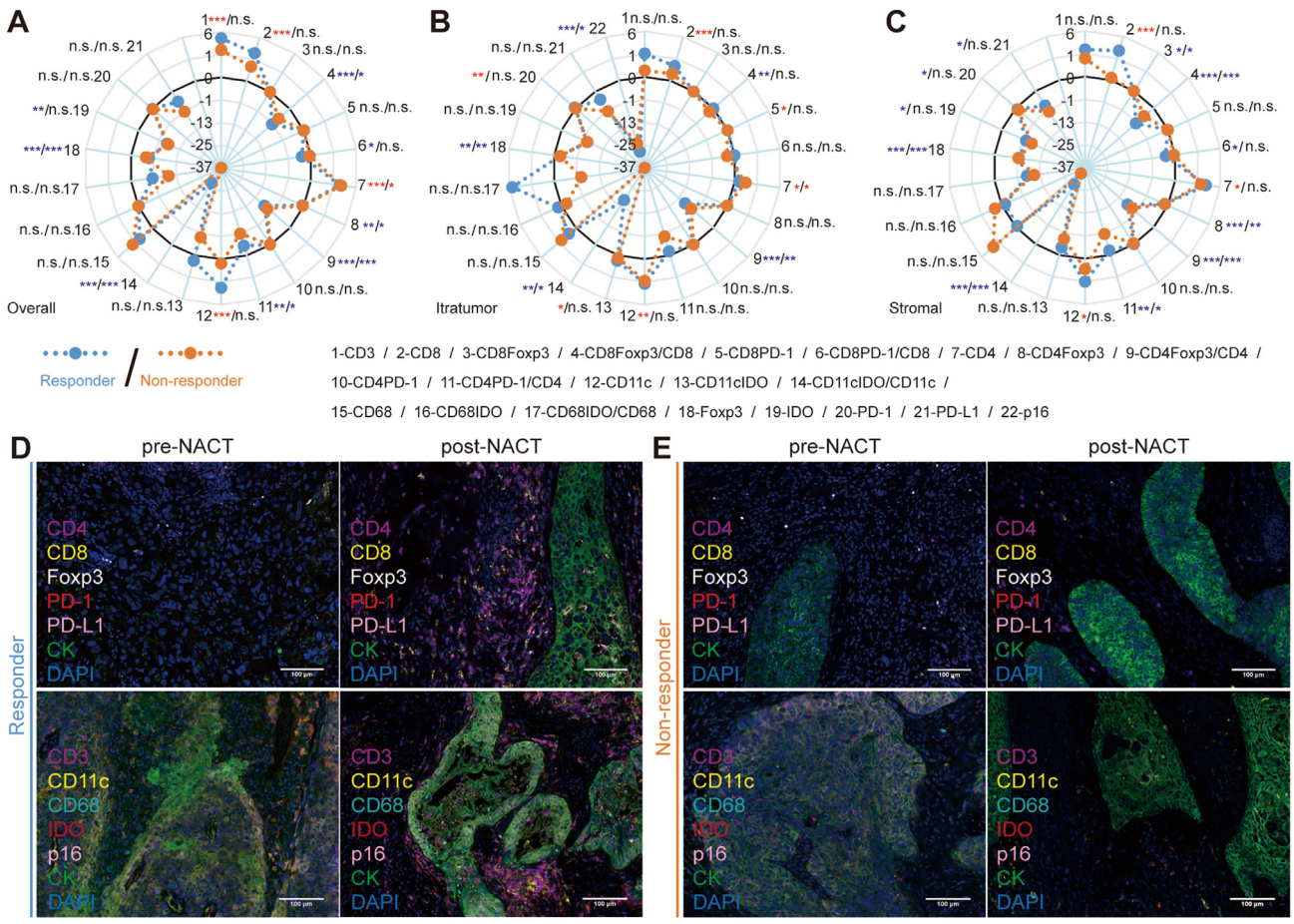

Figure 3. Changes in the tumor immune microenvironment were more evident in neoadjuvant chemotherapy (NACT) responders than in non-responders. The change of immune markers in pre- and post-NACT tumor samples across the (A) overall, (B) intratumor, and (C) stromal regions among clinical responders and non-responders. Each marker is shown with the change from pre-to post-NACT tumor samples, and statistical significance was determined using the Wilcoxon signed-rank test. n.s. $P \geq 0.05$, $^{*}P < 0.05$, $^{**}P < 0.01$, $^{***}P < 0.001$. The red marks represent a significant increase, while the blue marks represent a significant decrease in infiltration. Responder (left), non-responder (right). Representative images of multiplex staining in paired pre- and post-NACT cervical cancer samples from (D) responders and (E) non-responders. CD: Cluster of differentiation; CK: Cytokeratin; DAPI: 4′,6-Diamidino-2-phenylindole; Foxp3: Forkhead box P3; IDO: Indoleamine 2,3-dioxygenase; NACT: Neoadjuvant chemotherapy; n.s.: Non-significant; p16: Cyclin-dependent kinase inhibitor 2A; PD-1: Programmed cell death 1; PD-L1: Programmed cell death 1 ligand 1.

and processing cells around tumor cells in all patients. Moreover, more $CD3^{+}$ and $CD8^{+}$ T cells in chemotherapy-sensitive patients aggregated around tumor cells, indicating that the activation of tumor-reactive T cells by chemotherapy was possibly related to the killing effect of chemotherapeutic drugs on tumor cells.

Neoadjuvant chemotherapy enhances the contact between dendritic and T cells

We found that post-NACT, $Foxp3^{+}$ Tregs decreased and diverged from the tumor cells while dendritic cells increased and approached them, all possibly regulating the activation of effector T cells. We subsequently explored the interactions between $CD3^{+}$ and $CD8^{+}$ T cells and other immune cell groups. NACT intensified the contact between $CD3^{+}$ T and dendritic cells, manifesting as a narrowing distance between the two cell types (from 83 to 59 μm) [Figure 5A] and an increase in the dendritic cells within a 50-μm-radius of $CD3^{+}$ T cells [Figure 5B]. The dendritic cells responsible for antigen presentation suggestively interact more closely with T cells. Similarly, NACT dispersed the distribution and suitably reduced Tregs quantity around $CD8^{+}$ T cells [Figure 5C and D], relieving their dampening role on the killing function of $CD8^{+}$ T cells.

Similarly, NACT induced more dendritic cells clustering closer to $CD3^{+}$ T cells in responders and not in non-responders [Figure 5E and F], while Tregs decreased and moved further from $CD8^{+}$ T cells in responders and non-responders [Figure 5G and H]. These results show that NACT can effectively reduce Tregs in the local TIME and augment the contact between dendritic cells specializing in antigen presentation and $CD3^{+}$ T cells after effectively killing tumor cells, implying that antigen presentation may be enhanced during chemotherapy.

Enhancement of major histocompatibility complex antigen presentation reconstructs antitumor immunity in cervical cancer after neoadjuvant chemotherapy

To explore the possible mechanism of antitumor immunity triggered by NACT, we performed RNA-seq on four matched pre- and post-NACT tumor samples (the details of patients in Supplementary Table 3). Consistently, NACT upregulated the expression levels of CD3, CD8, and CD4 and downregulated those of Foxp3, PD-L1, IDO, and p16 [Figure 6A]. Moreover, the CIBERSORT algorithm revealed the expansion of $CD8^{+}$ T cell subsets in most residual lesions [Figure 6B]. We previously found that effectively killing tumor cells in responders strengthens the interaction between dendritic and $CD3^{+}$ T cells, implying that antigen presentation may be enhanced during effective chemotherapy. Further analysis using RNA-seq data revealed the activation of antigen receptor-mediated signaling and other immune-related pathways after NACT [Figure 6C] and a crucial increased expression of MHC I and MHC II, which are expressed at the cell surface and are involved in

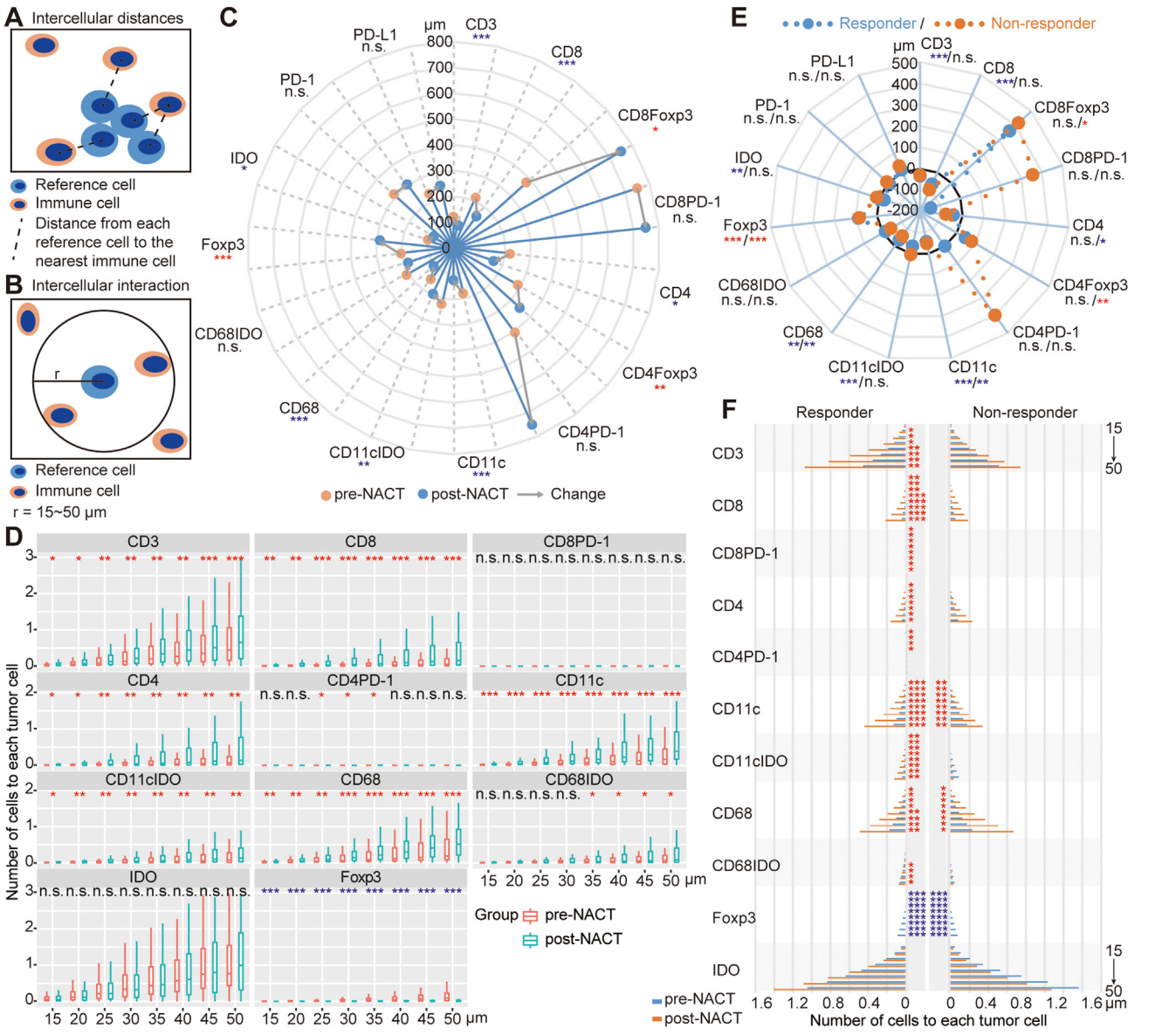

Figure 4. Antitumor immune cells were closer to tumor cells after neoadjuvant chemotherapy (NACT). (A) A schematic illustration of the average distance between the reference and immune cells. (B) A schematic illustration of density analysis of immune cells within 15–50 μm around a reference cell. (C) Median distances of tumor cells to different immune cells. (D) The density of immune cells within a 15–50-μm-radius of each tumor cell. (E) The change in average distances between different immune cells and the tumor cells upon NACT among responders and non-responders. Responder (left), non-responder (right). (F) The density of immune cells within a 15–50-μm-radius of each tumor cell among responders and non-responders. Statistical significance was determined using the Wilcoxon signed-rank test. n.s. $P \geq 0.05$, *$P < 0.05$, **$P < 0.01$, ***$P < 0.001$. The red marks represent a significant increase, while the blue marks represent a significant decrease in distances or density. Notes: The densities of $CD8^+Foxp3^+$ and $CD4^+Foxp3^+$ cells within a 15–50-μm-radius of each tumor cell were too low to show the comparison. CD: Cluster of differentiation; Foxp3: Forkhead box P3; IDO: Indoleamine 2,3-dioxygenase; NACT: Neoadjuvant chemotherapy; n.s.: Non-significant; PD-1: Programmed cell death 1; PD-L1: Programmed cell death 1 ligand 1.

antigen presentation [Supplementary Table 4]. Subsequently, we leveraged the IHC data of 41 matched pre- and post-NACT samples to validate the enhanced antigen presentation observed in cervical cancer [Figure 6D; patient details in Supplementary Table 5]. As shown in Figure 6E, NACT upregulated the overall expression of MHC I and MHC II. Most patients (MHC I, 75.6%; MHC II, 70.7%) showed stronger expression of MHC molecules post-NACT [Figure 6F]. The upregulation of MHC I and MHC II was more pronounced in responders than in non-responders (median of differences of MHC I in responders: 3.5, non-responders: 2.3; MHC II in responders: 3.1, non-responders: 2.3. Figure 6G and H); and more significant changes in MHC I in the intratumor than in the stromal region (median of differences of MHC I in intratumor: 2.7, stromal: 1.7; MHC II in intratumor: 1.7, stromal: 2.7. Figure 6I and J). These results suggest that NACT can stimulate antitumor immunity by enhancing antigen presentation in patients with cervical cancer.

Discussion

This study systematically identified the immunosuppressive tumor microenvironment of pre-NACT cervical cancer, which was reversed by platinum-based NACT. We found that the proportion of $CD8^+$ cytotoxic T cells was only 0.73% in the treatment-naive cervical cancer microenvironment, and immunosuppression was the primary manifestation. Post-NACT, Tregs were reduced and diverged from tumor cells, and the change of $CD8^+$ T cell infiltration was related to clinical response; that is, the infiltration of $CD3^+$ and $CD8^+$ T cells increased significantly in responders and not in non-responders. However, NACT did not affect $CD8^+$

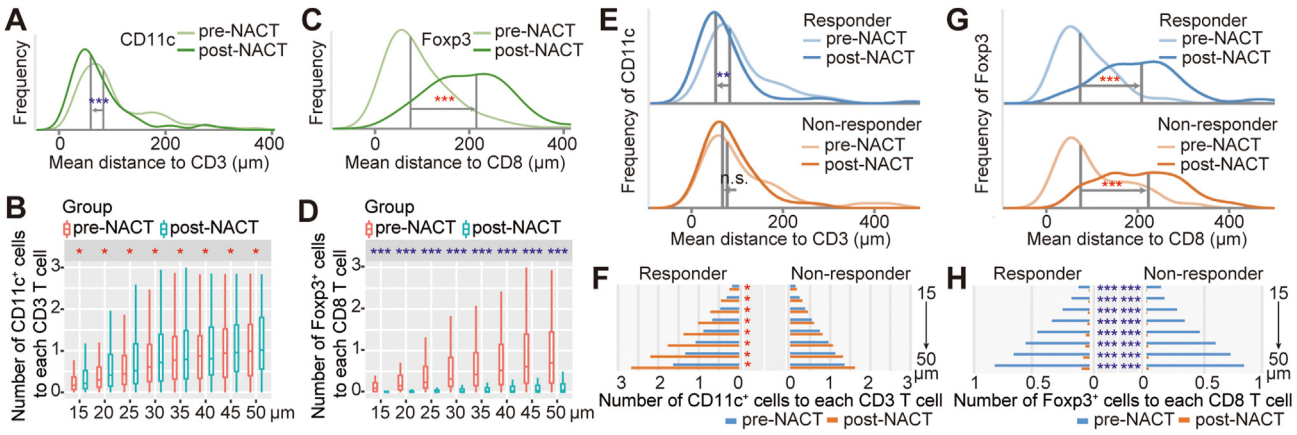

Figure 5. Neoadjuvant chemotherapy (NACT) promoted the interaction between the cluster of differentiation 11c$^+$ dendritic and the cluster of differentiation 3$^+$ T cells. Histograms showing the mean distances between (A) CD3$^+$ T and CD11c$^+$ cells and between (C) CD8$^+$ T and Foxp3$^+$ cells. The density of immune cells within a 15–50-μm-radius of each (B) CD3$^+$ T cell and (D) CD8$^+$ T cell. Histograms showing the mean distances between (E) CD3$^+$ T and CD11c$^+$ cells and between (G) CD8$^+$ T and Foxp3$^+$ cells among responders and non-responders. The density of immune cells within a 15–50-μm-radius of each (F) CD3$^+$ T cell and (H) CD8$^+$ T cell among responders and non-responders. n.s. $P \geq 0.05$, *$P < 0.05$, **$P < 0.01$, ***$P < 0.001$. The red marks represent a significant increase, while the blue marks represent a significant decrease in distance or density. CD: Cluster of differentiation; Foxp3: Forkhead box P3; NACT: Neoadjuvant chemotherapy; n.s.: Non-significant.

T cell exhaustion or PD-L1 expression in the tumor region. The local antigen presentation, including the function of dendritic cells and the expression of MHC molecules, was significantly enhanced in responders, which was considered the mechanism of antitumor immune activation. Nevertheless, local antitumor immunity remained weak post-NACT, particularly in NACT-resistant patients, who primarily lack activated immune and effector T cells. Our study provides a theoretical foundation that patients may benefit more from antitumor immunotherapy after chemotherapy.

As tissues become cancerous, they undergo immune editing to form immunosuppressive or immune desert microenvironments.[31] Many studies have explored and revealed different characteristics of local TIME from various tissues.[32] In this study, we combined the mIHC and spatial distribution analysis to accurately depict the complex tumor microenvironment of immune infiltration in 108 paired pre- and post-NACT cervical cancer samples of the International Federation of Gynecology and Obstetrics (FIGO) IB3-IIIA from two hospitals. Similarly, we assessed T cells, dendritic cells, and macrophages and their subsets with different functions and PD-1/PD-L1 and IDO immune checkpoint molecules. The infiltration rates of CD3$^+$ pan T and CD8$^+$ cytotoxic T cells in cervical cancer were 6.69% and 0.73%, respectively, while that of CD4$^+$ helper T cells was 1.14%. Moreover, most immune cells were present in the stromal rather than the intratumor region in our 108 cervical cancer tissues, suggesting that cervical cancer remains a tumor lacking antitumor immunity. More importantly, spatial results showed that CD8$^+$ T cells were far from tumor cells with a median distance of 214 μm; therefore, they could barely exert cytotoxic effects on tumor cells in pre-chemotherapy situations. Treatment-naive cervical cancer has an *in situ* immune-deprived microenvironment.

Evidence suggests that chemotherapy can exert varying local immunomodulatory functions in different tumors.[33] We found that the expression levels of CD3 and CD8 increased significantly in NACT-treated tumors, particularly in the stromal region of responders. Combined with spatial distribution analysis, CD8$^+$ T cells within 15–50 μm of tumor cells increased post-NACT, indicating that expanded CD8$^+$ T cells have antitumor effects, reflecting antitumor immune activation after NACT. However, NACT did not influence CD8$^+$ T cell exhaustion in the intratumor region regardless of the clinical response since the ratio of PD-1$^+$CD8$^+$ to CD8$^+$ T cells changed insignificantly, the same with PD-L1 expression, which is the indicator for ICIs. Despite the evident immune activation effect of NACT on cervical cancer, IDO$^+$ cells remained the primary subtype in NACT-treated samples. Notably, the enrichment of CD8$^+$ T cells was more intense in the stromal region and not evident in non-responders. Therefore, improving antitumor immunity post-NACT is possible, and immunotherapy can be used for patients after the therapy. Particularly for non-responders, more attention should be paid to supplementing effector T cells.

Chemotherapy is reportedly effective in reducing Tregs in the local TIME to induce protective anticancer immunity in various cancers, triggering a switch from a silent or ineffective to an overt or effective immune response.[22,34] In-depth research on cervical cancer remains lacking. In this study, we used more markers to analyze the subsets of Foxp3$^+$ cells and found that the infiltration of total, CD8$^+$, and CD4$^+$ Tregs decreased, and their distance from tumor cells increased in responders and non-responders. CD4$^+$ Tregs can effectively inhibit the biological activity of CD4$^+$ and CD8$^+$ T cells.[35] Although the effect of CD8$^+$ Tregs is less clear than that of CD4$^+$ Tregs, it is recognized as a subgroup of immunosuppressive cells.[36] Moreover, we found that NACT reduced the inhibitory action of Tregs on CD8$^+$ T cells. Therefore, our study showed that platinum-based NACT could significantly reduce local Tregs in cervical cancer, and this change was comparably evident in responders and non-responders, possibly related to the direct interaction of chemotherapeutic agents with immune cell subsets and selective depletion of immunosuppressive cells via immunogenic cell death-independent mechanisms.[22] Further research is needed to elucidate the complex and in-depth regulation of Tregs. Similarly, NACT downregulates the overall IDO and upregulates IDO$^+$ cells adjacent to tumor cells, including IDO-expressing dendritic cells and macrophages; therefore, a treatment combination with therapeutic inhibitors targeting IDO may be effective.[37] NACT can effectively reduce local Tregs, providing a theoretical basis for combining immunotherapy and chemotherapy.

Furthermore, we found that the increasing infiltration of CD3$^+$ and CD8$^+$ T cells and their reinforced contact with tumor cells primarily occurred in NACT-sensitive patients, indicating that activating antitumor immunity may partially depend on chemotherapy-induced tumor cell death. Previous studies have reported that chemotherapeutic drugs can activate antitumor immunity by promoting antigen exposure in specific tumor types;[38,39] however, this requires further validation in large clinical samples. In our study, among the responders, dendritic cells gathered around the tumor cells and were closely connected with CD3$^+$ T cells, indicating that antigen presentation by dendritic cells is crucial in activating antitumor immunity. The RNA-seq results further proved that post-NACT, various immune-related pathways, particularly that of antigen receptor-mediated signaling, were activated, and the mRNA level of

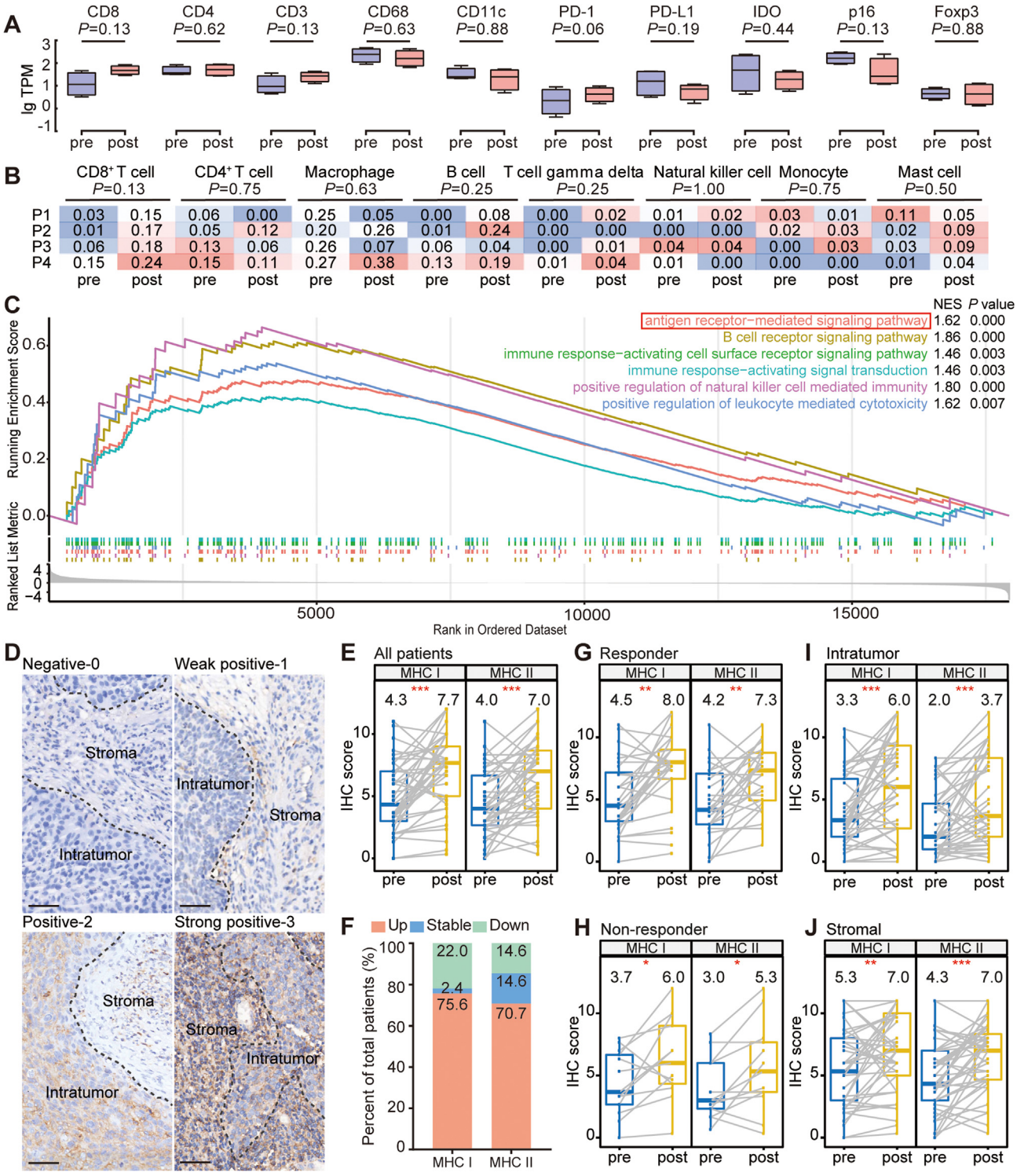

Figure 6. Gain of major histocompatibility complex (MHC) antigen presentation following neoadjuvant chemotherapy (NACT). Relative expression levels of the indicated genes were measured using RNA-seq in paired pre-NACT ($n = 4$) and post-NACT ($n = 4$) cervical tumor samples. (B) The relative abundance of diverse immune cell infiltrates was estimated through CIBERSORT analysis using the RNA-seq data. (C) Immune-related pathways were evaluated using gene set enrichment analysis. (D) Representative images of immunohistochemistry staining with different intensity scores. Scale bar, 50 μm. Relative levels of IHC score in paired pre- and post-NACT cervical tumor samples among (E) all patients ($n = 41$), (G) responders ($n = 28$), (H) non-responders ($n = 13$), (I) the intratumor region ($n = 41$), and (J) the stromal region ($n = 41$). $^*P < 0.05$, $^{**}P < 0.01$, $^{***}P < 0.001$. (F) Proportion of patients with different changes ($n = 41$). Up, higher IHC score; Stable, equal IHC score; Down, lower IHC score after NACT. CD: Cluster of differentiation; Foxp3: Forkhead box P3; IDO: Indoleamine 2,3-dioxygenase; IHC: Immunohistochemistry; MHC: Major histocompatibility complex; NES: Normalized enrichment score; p16: Cyclin-dependent kinase inhibitor 2A; PD-1: Programmed cell death 1; PD-L1: Programmed cell death 1 ligand 1; RNA-seq: Ribonucleic sequencing.

the MHC family was significantly upregulated. As reported in the literature, downregulation of MHC, indicating decreased antigen exposure and antigen presentation in cervical cancer, is a mechanism of immune escape and formation of an immunosuppressive microenvironment.[40] Our IHC results showed that MHC I and MHC II molecules were upregulated in cervical cancer following NACT treatment and that the change was more significant in responders. This was consistent with the result that dendritic cells were more enriched in the intratumor region and more closely contacted with $CD3^+$ T cells in responders post-NACT. These findings further demonstrate that in responders, chemotherapy can increase tumor antigen exposure and antigen presentation, activating antitumor immunity. In non-responders, chemotherapy promoted dendritic cell proximity to tumor cells within 50 μm and increased MHC I and MHC II, but not as significantly as in responders. Moreover, as dendritic cells did not increase in the intratumor or stromal regions or within 50 μm of T cells, antigen presentation was weak compared with those of responders, and chemotherapy failed to promote $CD8^+$ T cell infiltration effectively. Our study confirmed that NACT promotes the dendritic cell-mediated cross-presentation of tumor antigens to $CD8^+$ T lymphocytes concerning potent immunostimulatory cues, a mechanism by which chemotherapy stimulates antitumor immunity in responders.

This study revealed that treatment-naive cervical cancer lacks immune cell infiltration, whereas platinum-based NACT can significantly reduce Tregs, and enhance antigen presentation in responders, subsequently promoting $CD8^+$ and $CD4^+$ T cell infiltration. This provides a theoretical basis for immunotherapy timing; that is, immunotherapy applied after chemotherapy may benefit patients more. Moreover, NACT-resistant patients experienced significantly decreased immunosuppressive cells, similar to NACT-sensitive patients; however, no evident changes in the number or location of immune cells related to activated immunity and effector T cells, offering a novel immunotherapy direction for NACT-resistant patients. Our research provides a theoretical foundation for applying immunotherapy independently or combined with chemotherapy for cervical cancer and could offer novel ideas for treating cervical cancer. However, our findings are based on retrospective multicenter data, and more prospective studies are needed to supplement and verify them.

Funding

This study was supported by the National Clinical Research Center for Obstetrics and Gynecology (No. 2015BAI13B05), the National Key Technology Research and Development Program of China (Nos. 2022YFC2704400, 2022YFC2704403), and the National Natural Science Foundation of China (No. 81802896).

Authors contribution

Xue Feng, Xiaolin Meng, and Dihong Tang performed the experiments, analyzed data, and drafted the manuscript. Shuaiqingying Guo, Qiuyue Liao, Jing Chen, Qin Xie, and Fengyuan Liu coordinated the research and experiments. Yong Fang and Chaoyang Sun provided data analysis. Kezhen Li, Jihui Ai, and Yingyan Han were responsible for the study design and manuscript revision. All authors have read and approved the final manuscript.

Ethics statement

The study was approved by the Ethics Committee of Tongji Hospital (No. TJ-IRB20190322). Written informed consent was obtained from each patient.

Data availability statement

The data generated in this study are available upon reasonable request from the corresponding author. All raw RNA-seq data are publicly available in National Center for Biotechnology Information Sequence Read Archive under accession number SRP405747.

Conflict of interest

None.

Acknowledgments

None.

Appendix A. Supplementary data

Supplementary data to this article can be found online at https://doi.org/10.1016/j.cpt.2023.07.003.

References

1. Zhang Y, Zhang Z. The history and advances in cancer immunotherapy: understanding the characteristics of tumor-infiltrating immune cells and their therapeutic implications. *Cell Mol Immunol*. 2020;17:807–821. https://doi.org/10.1038/s41423-020-0488-6.
2. Mortezaee K. Immune escape: a critical hallmark in solid tumors. *Life Sci*. 2020;258:118110. https://doi.org/10.1016/j.lfs.2020.118110.
3. Salles G, Barrett M, Foà R, et al. Rituximab in B-cell hematologic malignancies: a review of 20 years of clinical experience. *Adv Ther*. 2017;34:2232–2273. https://doi.org/10.1007/s12325-017-0612-x.
4. Xin Yu J, Hodge JP, Oliva C, Neftelinov ST, Hubbard-Lucey VM, Tang J. Trends in clinical development for PD-1/PD-L1 inhibitors. *Nat Rev Drug Discov*. 2020;19:163–164. https://doi.org/10.1038/d41573-019-00182-w.
5. June CH, O'Connor RS, Kawalekar OU, Ghassemi S, Milone MC. CAR T cell immunotherapy for human cancer. *Science*. 2018;359:1361–1365. https://doi.org/10.1126/science.aar6711.
6. Ansell SM, Lesokhin AM, Borrello I, et al. PD-1 blockade with nivolumab in relapsed or refractory Hodgkin's lymphoma. *N Engl J Med*. 2015;372:311–319. https://doi.org/10.1056/NEJMoa1411087.
7. Eroglu Z, Zaretsky JM, Hu-Lieskovan S, et al. High response rate to PD-1 blockade in desmoplastic melanomas. *Nature*. 2018;553:347–350. https://doi.org/10.1038/nature25187.
8. Henriksen A, Dyhl-Polk A, Chen I, Nielsen D. Checkpoint inhibitors in pancreatic cancer. *Cancer Treat Rev*. 2019;78:17–30. https://doi.org/10.1016/j.ctrv.2019.06.005.
9. Rebuzzi SE, Rescigno P, Catalano F, et al. Immune checkpoint inhibitors in advanced prostate cancer: current data and future perspectives. *Cancers*. 2022;14:1245. https://doi.org/10.3390/cancers14051245.
10. Salmon H, Remark R, Gnjatic S, Merad M. Host tissue determinants of tumour immunity. *Nat Rev Cancer*. 2019;19:215–227. https://doi.org/10.1038/s41568-019-0125-9.
11. Lei X, Lei Y, Li JK, et al. Immune cells within the tumor microenvironment: biological functions and roles in cancer immunotherapy. *Cancer Lett*. 2020;470:126–133. https://doi.org/10.1016/j.canlet.2019.11.009.
12. Cohen PA, Jhingran A, Oaknin A, Denny L. Cervical cancer. *Lancet*. 2019;393:169–182. https://doi.org/10.1016/S0140-6736(18)32470-X.
13. Sung H, Ferlay J, Siegel RL, et al. Global Cancer Statistics 2020: GLOBOCAN estimates of incidence and mortality worldwide for 36 cancers in 185 countries. *Ca - Cancer J Clin*. 2021;71:209–249. https://doi.org/10.3322/caac.21660.
14. Tewari KS, Sill MW, Penson RT, et al. Bevacizumab for advanced cervical cancer: final overall survival and adverse event analysis of a randomised, controlled, open-label, phase 3 trial (Gynecologic Oncology Group 240). *Lancet*. 2017;390:1654–1663. https://doi.org/10.1016/S0140-6736(17)31607-0.
15. Shamseddine AA, Burman B, Lee NY, Zamarin D, Riaz N. Tumor immunity and immunotherapy for HPV-related cancers. *Cancer Discov*. 2021;11:1896–1912. https://doi.org/10.1158/2159-8290.Cd-20-1760.
16. Stevanovic S, Draper LM, Langhan MM, et al. Complete regression of metastatic cervical cancer after treatment with human papillomavirus-targeted tumor-infiltrating T cells. *J Clin Oncol*. 2015;33:1543–1550. https://doi.org/10.1200/JCO.2014.58.9093.
17. Mauricio D, Zeybek B, Tymon-Rosario J, Harold J, Santin AD. Immunotherapy in cervical cancer. *Curr Oncol Rep*. 2021;23:61. https://doi.org/10.1007/s11912-021-01052-8.
18. Zhu S, Zhang T, Zheng L, et al. Combination strategies to maximize the benefits of cancer immunotherapy. *J Hematol Oncol*. 2021;14:156. https://doi.org/10.1186/s13045-021-01164-5.
19. Provencio M, Serna-Blasco R, Nadal E, et al. Overall survival and biomarker analysis of neoadjuvant nivolumab plus chemotherapy in operable stage IIIA non-small-cell lung cancer (NADIM phase II trial). *J Clin Oncol*. 2022;40:2924–2933. https://doi.org/10.1200/JCO.21.02660.
20. Miles D, Gligorov J, Andre F, et al. Primary results from IMpassion131, a double-blind, placebo-controlled, randomised phase III trial of first-line paclitaxel with or without atezolizumab for unresectable locally advanced/metastatic triple-negative

breast cancer. *Ann Oncol*. 2021;32:994–1004. https://doi.org/10.1016/j.annonc.2021.05.801.
21. Colombo N, Dubot C, Lorusso D, et al. Pembrolizumab for persistent, recurrent, or metastatic cervical cancer. *N Engl J Med*. 2021;385:1856–1867. https://doi.org/10.1056/NEJMoa2112435.
22. Galluzzi L, Humeau J, Buque A, Zitvogel L, Kroemer G. Immunostimulation with chemotherapy in the era of immune checkpoint inhibitors. *Nat Rev Clin Oncol*. 2020;17:725–741. https://doi.org/10.1038/s41571-020-0413-z.
23. Zhang Y, Yu M, Jing Y, et al. Baseline immunity and impact of chemotherapy on immune microenvironment in cervical cancer. *Br J Cancer*. 2021;124:414–424. https://doi.org/10.1038/s41416-020-01123-w.
24. Liang Y, Lu W, Zhang X, Lu B. Tumor-infiltrating CD8+ and FOXP3+ lymphocytes before and after neoadjuvant chemotherapy in cervical cancer. *Diagn Pathol*. 2018;13:93. https://doi.org/10.1186/s13000-018-0770-4.
25. Fu T, Dai LJ, Wu SY, et al. Spatial architecture of the immune microenvironment orchestrates tumor immunity and therapeutic response. *J Hematol Oncol*. 2021;14:98. https://doi.org/10.1186/s13045-021-01103-4.
26. Tsujikawa T, Mitsuda J, Ogi H, et al. Prognostic significance of spatial immune profiles in human solid cancers. *Cancer Sci*. 2020;111:3426–3434. https://doi.org/10.1111/cas.14591.
27. Barua S, Fang P, Sharma A, et al. Spatial interaction of tumor cells and regulatory T cells correlates with survival in non-small cell lung cancer. *Lung Cancer*. 2018;117:73–79. https://doi.org/10.1016/j.lungcan.2018.01.022.
28. Eisenhauer EA, Therasse P, Bogaerts J, et al. New response evaluation criteria in solid tumours: revised RECIST guideline (version 1.1). *Eur J Cancer*. 2009;45:228–247. https://doi.org/10.1016/j.ejca.2008.10.026.
29. Li T, Fu J, Zeng Z, et al. TIMER2.0 for analysis of tumor-infiltrating immune cells. *Nucleic Acids Res*. 2020;48:W509–W514. https://doi.org/10.1093/nar/gkaa407.
30. Schwen LO, Andersson E, Korski K, et al. Data-driven discovery of immune contexture biomarkers. *Front Oncol*. 2018;8:627. https://doi.org/10.3389/fonc.2018.00627.
31. Ferrall L, Lin KY, Roden RBS, Hung CF, Wu TC. Cervical cancer immunotherapy: facts and hopes. *Clin Cancer Res*. 2021;27:4953–4973. https://doi.org/10.1158/1078-0432.Ccr-20-2833.
32. Thorsson V, Gibbs DL, Brown SD, et al. The immune landscape of cancer. *Immunity*. 2018;48:812–830. https://doi.org/10.1016/j.immuni.2018.03.023.
33. van den Ende T, van den Boorn HG, Hoonhout NM, et al. Priming the tumor immune microenvironment with chemo(radio)therapy: a systematic review across tumor types. *Biochim Biophys Acta Rev Cancer*. 2020;1874:188386. https://doi.org/10.1016/j.bbcan.2020.188386.
34. Galluzzi L, Buqué A, Kepp O, Zitvogel L, Kroemer G. Immunological effects of conventional chemotherapy and targeted anticancer agents. *Cancer Cell*. 2015;28:690–714. https://doi.org/10.1016/j.ccell.2015.10.012.
35. Shevach EM, Thornton AM. tTregs, pTregs, and iTregs: similarities and differences. *Immunol Rev*. 2014;259:88–102. https://doi.org/10.1111/imr.12160.
36. Fattorossi A, Battaglia A, Ferrandina G, et al. Neoadjuvant therapy changes the lymphocyte composition of tumor-draining lymph nodes in cervical carcinoma. *Cancer*. 2004;100:1418–1428. https://doi.org/10.1002/cncr.20130.
37. Prendergast GC, Malachowski WJ, Mondal A, Scherle P, Muller AJ. Indoleamine 2,3-dioxygenase and its therapeutic inhibition in cancer. *Int Rev Cell Mol Biol*. 2018;336:175–203. https://doi.org/10.1016/bs.ircmb.2017.07.004.
38. Gravett AM, Trautwein N, Stevanovic S, Dalgleish AG, Copier J. Gemcitabine alters the proteasome composition and immunopeptidome of tumour cells. *OncoImmunology*. 2018;7:e1438107. https://doi.org/10.1080/2162402X.2018.1438107.
39. Liu WM, Fowler DW, Smith P, Dalgleish AG. Pre-treatment with chemotherapy can enhance the antigenicity and immunogenicity of tumours by promoting adaptive immune responses. *Br J Cancer*. 2010;102:115–123. https://doi.org/10.1038/sj.bjc.6605465.
40. Rock KL, Reits E, Neefjes J. Present yourself! By MHC class I and MHC class II molecules. *Trends Immunol*. 2016;37:724–737. https://doi.org/10.1016/j.it.2016.08.010.